

Energy extraction via magnetic reconnection in magnetized black holes

Shao-Jun Zhang^{1,2,*}

¹*Institute for Theoretical Physics and Cosmology, Zhejiang*

University of Technology, Hangzhou 310032, China

²*United Center for Gravitational Wave Physics, Zhejiang University of Technology, Hangzhou 310032, China*

(Dated: May 31, 2024)

The Comisso-Asenjo mechanism is a novel mechanism proposed recently to extract energy from black holes through magnetic reconnection of the surrounding charged plasma, in which the magnetic field plays a crucial role. In this work, we revisit this process by taking into account the backreaction of the magnetic field on the black hole's geometry. We employ the Kerr-Melvin metric to describe the local near-horizon geometry of the magnetized black hole. By analyzing the circular orbits in the equatorial plane, energy extraction conditions, power and efficiency of the energy extraction, we found that while a stronger magnetic field can enhance plasma magnetization and aid energy extraction, its backreaction on the spacetime may hinder the process, with a larger magnetic field posing a greater obstacle. Balancing these effects, an optimal moderate magnetic field strength is found to be most conducive to energy extraction. Moreover, there is a maximum limit to the magnetic field strength associated with the black hole's spin, beyond which circular orbits in the equatorial plane are prohibited, thereby impeding energy extraction in the current scenario.

I. INTRODUCTION

Black holes, known as the most compact and unique objects envisioned by Einstein's gravitational theory, are believed to play a crucial role in various high-energy astrophysical phenomena, such as gamma-ray bursts (GRBs) and relativistic jets observed in active galactic nuclei (AGNs). The energy emitted in these occurrences can stem from either the gravitational potential energy discharged as material falls into the black hole or from the intrinsic energy of the black hole itself. According to general relativity (GR) and black hole thermodynamics, rotating black holes harbor significant amounts of extractable energy, with the potential to reach up to $0.29Mc^2$ [1], where M represents the black hole's mass and c denotes the speed of light in vacuum. This substantial energy arises from the rotational energy of the black hole, leading to an intriguing exploration of the mechanisms involved in harnessing such a considerable fraction of the black hole's energy.

* sjzhang@zjut.edu.cn

The first energy extraction mechanism was proposed by Penrose in 1969, and is now known as Penrose process [?]. This process entails the division of a particle within the ergoregion into two distinct particles. Despite its theoretical appeal, the Penrose process is deemed impractical due to the necessity for the newly formed particles to exhibit relative velocities exceeding half the speed of light, a scenario rarely observed in actual astrophysical phenomena [2, 3]. Penrose’s seminal work has spurred physicists to investigate various alternative mechanisms for extracting energy from black holes. These alternatives include collisional Penrose process [5], superradiant scattering [4], Blandford-Znajek (BZ) process [6], and magnetohydrodynamic (MHD) Penrose process [7]. Of these, the BZ process is currently recognized as the most promising method for interpreting GRBs [8–10] and relativistic jets in AGNs [11–14].

Recently, Comisso and Asenjo proposed a novel mechanism for extracting energy from black holes by utilizing magnetic reconnection processes within the ergoregion of a rotating black hole [15] (see also a prior exploratory study [16]). This mechanism involves the generation of anti-parallel magnetic field configurations near the equatorial plane due to the black hole’s rotation [17–20]. The magnetic field direction changes, forming current sheets that give rise to plasmoids through a disruptive plasmoid instability process [21–23]. These plasmoids facilitate rapid magnetic reconnection, converting magnetic energy into plasma kinetic energy before being expelled from the reconnection layer [24, 25]. The magnetic field lines are elongated by the black hole’s rotation, initiating the formation of new current sheets and repeating the reconnection process. During each reconnection event, the plasma in the current sheet splits into corotating and counterrotating components. The corotating part is accelerated, while the counterrotating part is decelerated. Analogous to Penrose process, energy extraction from the black hole is achieved by absorbing the decelerated portion carrying negative energy into the black hole, allowing the accelerated portion to escape with additional energy obtained from the black hole’s rotational energy.

Observations have verified the presence of diverse magnetic field scales surrounding black holes, supported by accretion matter or companion stars. In particular, the supermassive black hole Sagittarius A* is associated with the magnetar SGR J1745-2900, and a strong magnetic field is detected near the event horizon of the black hole in M87* [26–30]. The magnetic reconnection process in black holes is expected to be a common occurrence. Research by Comisso and Asenjo suggests that this mechanism may outperform the BZ process in specific circumstances, making it a promising avenue for extracting energy from black holes. Expanding on this fundamental research, the Comisso-Asenjo mechanism has been applied to various other rotating black holes and scenarios [31–41].

In all the mentioned work, the backreaction of the surrounding magnetic fields (and also the plasma) on the black hole geometry has been ignored, as they are typically considered insignificant compared to the black hole's gravitational energy. Nevertheless, recent astronomical observations have identified situations where the strength of magnetic fields in the universe necessitates a consideration of their influence on spacetime geometry [29, 30]. Further elaboration on the magnetic field surrounding black holes will be provided in the main text. In any case, it is always of theoretical interest to consider the backreaction of the magnetic field on the black hole geometry and, in turn, on the Comisso-Asenjo mechanism.

Inspired by these works, we reexamine the Comisso-Asenjo mechanism by incorporating the influence of the magnetic field's backreaction on the geometry of the black hole. Analyzing the dynamic interplay between black holes and surrounding magnetic fields is in general an intricate task, often requiring relativistic magnetohydrodynamic simulations. A more straightforward approach involves investigating stationary magnetized black hole solutions to establish fundamental insights. Notably, solutions to the Einstein-Maxwell equations, such as Kerr-Melvin black holes within a uniform magnetic field along the symmetry axis, have been identified in the literature [42–45]. Recent studies have delved into the thermodynamic properties and astrophysical implications of Kerr-Melvin black holes, contributing significantly to our understanding of these black holes [46–56]. We intend to utilize this simplified model to describe the local near-horizon geometry of the magnetized black holes, aiming to gain insights into the underlying physics. A thorough examination reveals that while increasing the magnetic field strength can improve plasma magnetization and aid in energy extraction, its influence on spacetime could impede the process, particularly with larger magnetic fields presenting a greater challenge.

The paper is organized as follows. In Section II, we give a brief overview of the Kerr-Melvin black holes, along with an examination of how the magnetic field affects the ergoregion. Section III delves into a thorough analysis of the circular geodesic motion of the plasma in the equatorial plane. Section IV investigates the energy extraction from the black holes via the Comisso-Asenjo mechanism. The last section is the summary and conclusions.

II. KERR-MELVIN BLACK HOLES

We consider the Kerr-Melvin metric, which is an exact stationary and axisymmetric electrovacuum solution describing a rotating black hole immersed in an external uniform magnetic field. The

metric takes the form [43–45, 51, 57, 58]

$$ds^2 = \Sigma |\Lambda|^2 \left[-\frac{\Delta}{A} dt^2 + \frac{dr^2}{\Delta} + d\theta^2 \right] + \frac{A \sin^2 \theta}{\Sigma |\Lambda|^2} (|\Lambda_0|^2 d\phi - \omega dt)^2, \quad (1)$$

where

$$\begin{aligned} \Delta &= r^2 + a^2 - 2Mr, & \Sigma &= r^2 + a^2 \cos^2 \theta, & A &= (r^2 + a^2)^2 - \Delta a^2 \sin^2 \theta, \\ \Lambda &= 1 + \frac{B^2 \sin^2 \theta A}{4 \Sigma} - \frac{i}{2} a B^2 M \cos \theta \left(3 - \cos^2 \theta + \frac{a^2 \sin^4 \theta}{\Sigma} \right), \\ \omega &= \frac{\alpha - \beta \Delta}{r^2 + a^2}, \\ \alpha &= a(1 - a^2 M^2 B^4), \\ \beta &= \frac{a \Sigma}{A} + \frac{a M B^4}{16} \left(-8r \cos^2 \theta (3 - \cos^2 \theta) - 6r \sin^4 \theta + \frac{2a^2 \sin^6 \theta}{A} [r(r^2 + a^2) + 2Ma^2] \right. \\ &\quad \left. + \frac{4Ma^2 \cos^2 \theta}{A} [(r^2 + a^2)(3 - \cos^2 \theta)^2 - 4a^2 \sin^2 \theta] \right). \end{aligned} \quad (2)$$

Here M and a are the black hole's mass and spin parameters respectively, and B is the asymptotic magnetic field strength. The additional factor $|\Lambda_0|^2 \equiv |\Lambda(\theta = 0)|^2 = 1 + a^2 M^2 B^4$ is introduced in the metric to remove the canonical singularities on the polar axis [57, 58]. Note the metric is not asymptotically flat but resembles the Melvin magnetic universe [59]. Nevertheless, we employ it to describe the local geometry near the black hole and assume that the spacetime is still asymptotically flat. We do not have to worry about the explicit geometry far away from the black hole as it is not relevant to the physics we are going to study.

When $B = 0$, the metric reduces to the Kerr metric exactly; when $a = 0$, it reduces to the Schwarzschild-Melvin metric [43]. The detailed electromagnetic field configuration expression, which is lengthy and not pertinent to this study, is omitted here. For more details, refer to [43–45, 51, 57, 58].

In this work, we utilize the units $c = G = 4\pi\epsilon_0 = 1$, where c, G, ϵ_0 are the speed of light in vacuum, the Newton gravitational constant and the vacuum permittivity, respectively. Moreover, it is convenient to set the black hole mass $M = 1$ so that all quantities are measured in units of M . In this convention, one can define a characteristic magnetic field $B_M = 1/M$ associated to a spacetime curvature of the same order of the horizon curvature. At this order, the electromagnetic energy is comparable to the gravitational energy of the black hole [58, 60]. Restoring physical units, we have

$$B_M \sim 2.36 \times 10^{19} \left(\frac{M_\odot}{M} \right) \text{ Gauss}, \quad (3)$$

where M_\odot is the solar mass. B_M is inversely proportional to the mass of the BH, and takes an extremely high value in general: For stellar-mass BHs with $M \sim 10M_\odot$, $B_M \sim 10^{18}$ Gauss; For intermediate-mass BHs with $M \sim 10^2M_\odot$, $B_M \sim 10^{17}$ Gauss; While for supermassive BHs with $M \sim 10^6M_\odot$ (for example the Sagittarius A*), $B_M \sim 10^{13}$ Gauss. Given that the most powerful magnetic field observed in the universe measures around $B \sim 10^{16}$ Gauss [29], B/B_M should not be presumed to be small. However, as we will see later, for the process we are going to study to happen, the magnetic field should not be too strong.

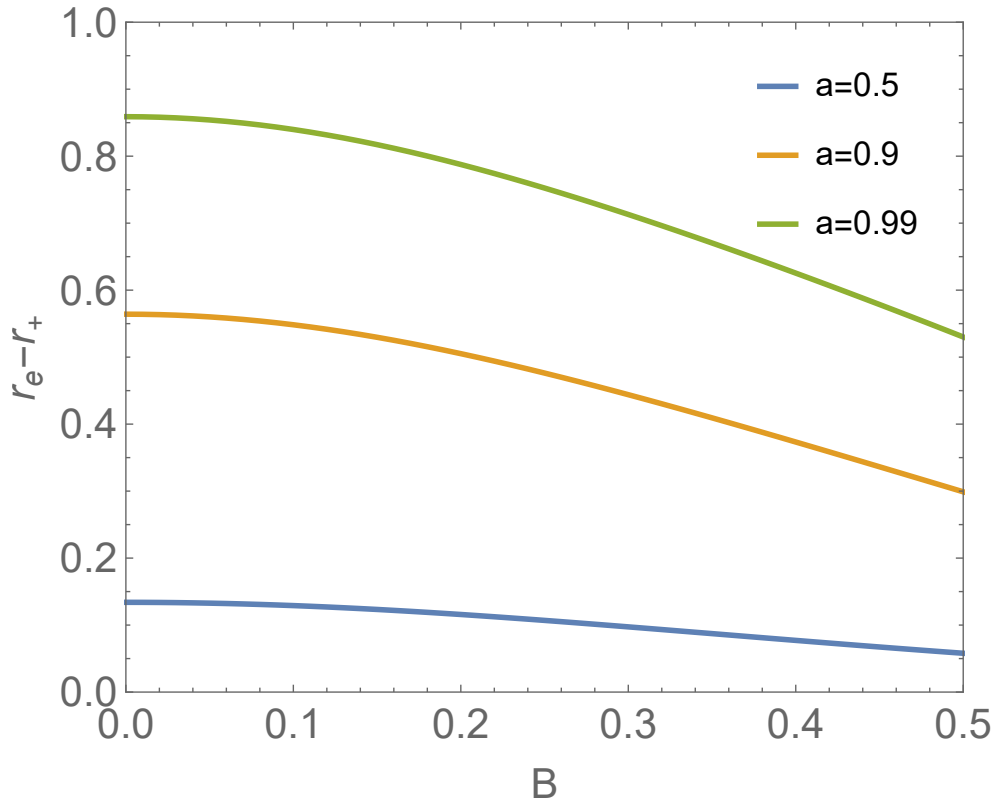


FIG. 1. Ergosphere in the equatorial plane as a function of the magnetic field strength B for various black hole spin a . All physical quantities are measured in units of M .

The location of the event horizon is not affected by the magnetic field and remains the same as that of the corresponding Kerr black hole, that is,

$$r_+ = M + \sqrt{M^2 - a^2}. \quad (4)$$

The radius of the ergosphere $r = r_e(\theta)$ is determined by the condition

$$g_{tt} = -\Sigma|\Lambda|^2\frac{\Delta}{A} + \frac{A\sin^2\theta}{\Sigma|\Lambda|^2}\omega^2 = 0. \quad (5)$$

The ergoregion is enclosed by the ergosphere and the event horizon, that is, $r_e > r > r_+$. In the limit of $B \rightarrow 0$, $r_e = M + \sqrt{M^2 - a^2 \cos^2 \theta}$. Our main focus in this work is on the ergoregion in the equatorial plane, i.e., $\theta = \frac{\pi}{2}$. In Fig. 1, we show the influence of the magnetic field on the shape of the ergoregion in the equatorial plane. From the figure, it can be seen that for a fixed black hole spin a , larger B will shrink the ergoregion. This implies that the backreaction of the magnetic field on spacetime is not conducive to the magnetic reconnection process.

III. CIRCULAR ORBITS IN EQUATORIAL PLANE

Magnetic reconnection is associated with the movement of charged plasma in the vicinity of the compact object. Under the "force-free" assumption, the net electromagnetic force on the charged plasma is neglected, and thus the particles move on geodesics. With the two Killing vectors of the spacetime, $k \equiv \partial_t$ and $m \equiv \partial_\phi$, one can define two associated conserved quantities for the particles, the specific energy $E \equiv -g_{\mu\nu} k^\mu u^\nu$ and the z -component angular momentum $L_z \equiv g_{\mu\nu} m^\mu u^\nu$, with $u^\mu \equiv \dot{x}^\mu$ being the four-velocity of the particle (where dot means derivative with respect to some affine parameter). From the normalization condition of the four-velocity of the particle, i.e., $g_{\mu\nu} \dot{x}^\mu \dot{x}^\nu = -1$, we have the equation [40]

$$g_{rr} \dot{r}^2 + g_{\theta\theta} \dot{\theta}^2 = V_{\text{eff}}(r, \theta), \quad (6)$$

where the effective potential $V_{\text{eff}}(r, \theta)$ can be written in terms of E and L_z as

$$V_{\text{eff}}(r, \theta) = \frac{g_{\phi\phi} E^2 + 2g_{t\phi} E L_z + g_{tt} L_z^2}{g_{t\phi}^2 - g_{tt} g_{\phi\phi}} - 1. \quad (7)$$

For circular orbits in the equatorial plane, i.e., $\theta = \frac{\pi}{2}$, $\dot{\theta} = 0$ and $\dot{r} = 0$, the effective potential should satisfy the following conditions

$$V_{\text{eff}} = 0, \quad \partial_r V_{\text{eff}} = 0, \quad \partial_\theta V_{\text{eff}} = 0. \quad (8)$$

The last condition can consistently be fulfilled due to the reflection symmetry of spacetime with respect to the equatorial plane. The first two conditions determine the Keplerian angular velocity $\Omega_K \equiv \dot{\phi}/\dot{t}$, the specific energy E , and the z -component angular momentum L_z of the particle as a

function of the radius of the circular orbit, that is [40]

$$\Omega_K = \frac{-\partial_r g_{t\phi} \pm \sqrt{(\partial_r g_{t\phi})^2 - (\partial_r g_{tt})(\partial_r g_{\phi\phi})}}{\partial_r g_{\phi\phi}}, \quad (9)$$

$$E = -\frac{g_{tt} + g_{t\phi}\Omega_K}{\sqrt{-g_{tt} - 2g_{t\phi}\Omega_K - g_{\phi\phi}\Omega_K^2}}, \quad (10)$$

$$L_z = \frac{g_{t\phi} + g_{\phi\phi}\Omega_K}{\sqrt{-g_{tt} - 2g_{t\phi}\Omega_K - g_{\phi\phi}\Omega_K^2}}, \quad (11)$$

where the sign + and - stands for corotating and counterrotating orbits, respectively.

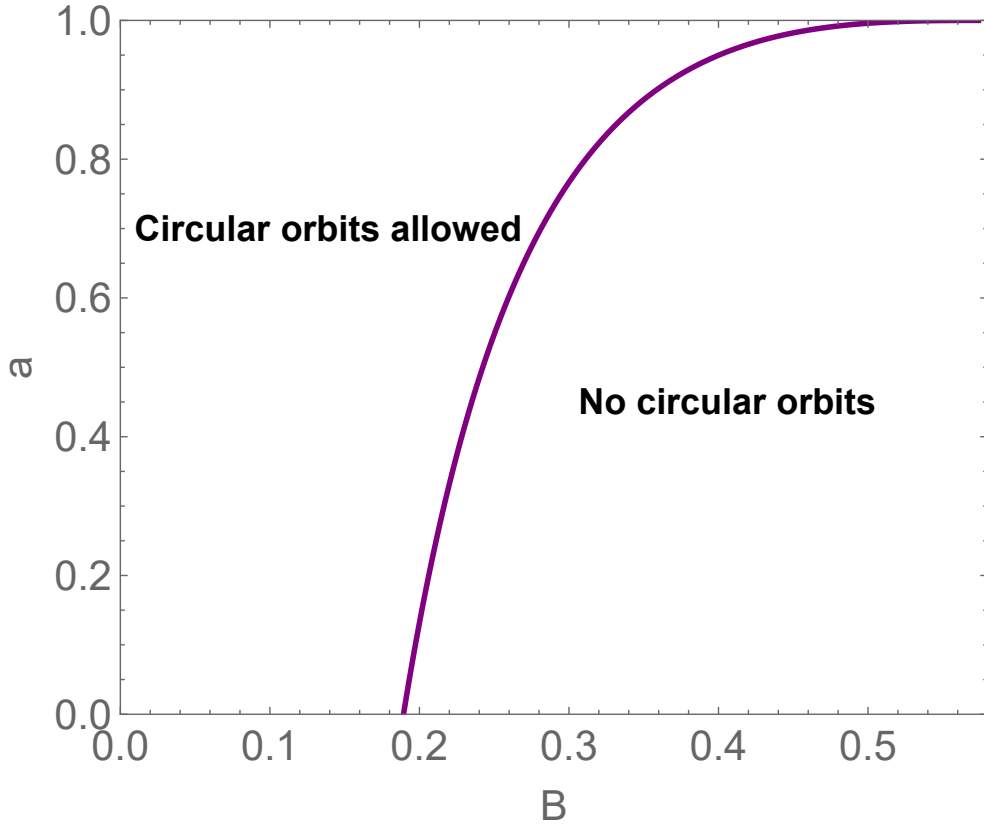


FIG. 2. Allowed region in the $B - a$ plane for the existence of circular orbits in the equatorial plane. The two endpoints of the curve are $(a, B) \sim (0, 0.19)$ and $(1, 0.57)$, respectively. All physical quantities are measured in units of M .

For circular orbits to exist, the above three orbital quantities (9) (10)(11) should be real, so expressions under the root must be nonnegative. This physical requirement gives us an allowed region in the $B - a$ plane, as shown in Fig. 2. For a given a , from the figure, it can be seen that there exists an upper limit of the magnetic field strength $B = B_c$ over which no circular orbits exist, and B_c increases along with the increase of a . In the non-rotating limit $a = 0$, $B_c \sim 0.19$;

While in the extremal limit $a \rightarrow 1$, B_c does not diverge but approaches a finite value $B_c \sim 0.57$. This result implies that if the magnetic field is too strong, the circular orbits are prohibited, and thus the physical process we are considering will not occur. So in the following, we only consider $B \lesssim 0.57$.

The counterrotating orbits are always outside the ergoregion, so we will only focus on the corotating ones. A radially stable circular orbit exists from infinity to the innermost (radially) stable circular orbit (ISCO), whose radius is determined by the condition

$$\partial_r^2 V_{\text{eff}} = 0. \quad (12)$$

In Fig. 3, we plot the radius of the corotating ISCO r_{ISCO}^+ as a function of a for various B . From it, one can see that only when a exceeds some extremely high value a_c can r_{ISCO}^+ enter the ergoregion. For example, $a_c \sim 0.943, 0.939, 0.934, 0.935$ for $B = 0, 0.1, 0.2, 0.3$, respectively. It can be seen that with the increase of B , a_c first decreases and then increases. In the extremal limit $a \rightarrow 1$, $r_{\text{ISCO}}^+ \rightarrow r_+$ for any B . We have also numerically verified that the vertically stable condition $\partial_\theta^2 V_{\text{eff}} \leq 0$ is consistent for the (radially) ISCO.

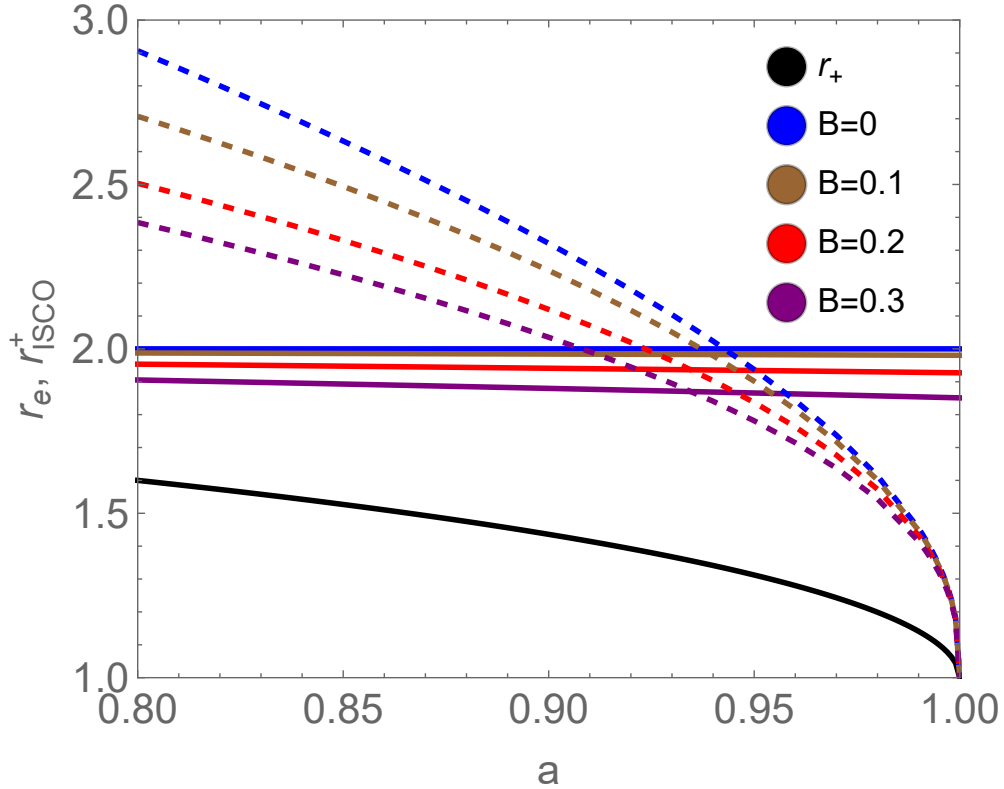


FIG. 3. Corotating ISCOs r_{ISCO}^+ as a function of a for various B . Black solid curve is r_+ , other solid ones are r_e , and dashed curves are r_{ISCO}^+ . All physical quantities are measured in units of M .

IV. ENERGY EXTRACTION VIA MAGNETIC RECONNECTION

The Comisso-Asenjo mechanism facilitates energy extraction from black holes through magnetic reconnection occurring within the charged plasma situated in the ergoregion. Following [15], we consider the plasma to rotate in a stable circular orbit in the equatorial plane at Keplerian velocity Ω_K . Under the assumption of the one-fluid approximation, the energy-momentum tensor of the plasma takes the form

$$T^{\mu\nu} = pg^{\mu\nu} + \omega_0 U^\mu U^\nu + F^\mu{}_\sigma F^{\nu\sigma} - \frac{1}{4} g^{\mu\nu} F^{\rho\sigma} F_{\rho\sigma}, \quad (13)$$

where p, ω_0, U^μ and $F^{\mu\nu}$ are the proper plasma pressure, enthalpy density, four-velocity, and electromagnetic field tensors, respectively. With the time-like killing vector $\chi = \partial_t$, one can define a covariant conserved energy current $J^\mu \equiv T^{\mu\nu} \chi_\nu$ and the associated energy density,

$$e^\infty \equiv n_\mu J^\mu = -\alpha g_{\mu 0} T^{\mu 0}, \quad (14)$$

where n^μ is the unit vector normal to time-like hypersurfaces $t = \text{constant}$. e^∞ is usually called the “energy-at-infinity” density.

To evaluate e^∞ , it is convenient to express it in terms of physical quantities in “zero-angular-momentum-observer” (ZAMO) frame ($\hat{t}, \hat{x}^1 = \hat{r}, \hat{x}^2 = \hat{\theta}, \hat{x}^3 = \hat{\phi}$) [2]. The ZAMO frame is a locally non-rotating frame in which the spacetime is locally Minkowskian, i.e., $ds^2 = -d\hat{t}^2 + \sum_{i=1}^3 (d\hat{x}^i)^2 = \eta_{\mu\nu} d\hat{x}^\mu d\hat{x}^\nu$. It is related to the Boyer-Lindquist coordinates ($t, x^1 = r, x^2 = \theta, x^3 = \phi$) by the transformations $d\hat{t} = \alpha dt$ and $d\hat{x}^i = \sqrt{g_{ii}} dx^i - \alpha \beta^i dt$, where the lapse function α and the shift vector $\beta^i = (0, 0, \beta^\phi)$ are

$$\alpha = \left(-g_{tt} + \frac{g_{t\phi}^2}{g_{\phi\phi}} \right)^{1/2}, \quad \beta^\phi = \frac{\sqrt{g_{\phi\phi}} \omega^\phi}{\alpha}, \quad (15)$$

and $\omega^\phi \equiv -g_{t\phi}/g_{\phi\phi}$ is the angular velocity of the frame dragging. Quantities in ZAMO frame are denoted with hats. The Keplerian velocity of the co-rotating bulk plasma in ZAMO frame becomes

$$\hat{v}_K = \frac{d\hat{x}^\phi}{d\hat{t}} = \frac{\sqrt{g_{\phi\phi}}}{\alpha} \Omega_K - \beta^\phi. \quad (16)$$

During each instance of magnetic reconnection, the plasma flowing out will divide into two segments, with one segment experiencing deceleration and the other acceleration. Assuming a significant conversion of magnetic energy to kinetic energy, allowing the electromagnetic energy density to be disregarded, and under the assumption of incompressible and adiabatic plasma, the

energy density per enthalpy at infinity for the two segments can be expressed as follows [15]

$$\epsilon_{\pm}^{\infty} = \alpha \hat{\gamma}_K \left[(1 + \beta^{\phi} \hat{v}_K)(1 + \sigma_0)^{1/2} \pm \cos \xi (\beta^{\phi} + \hat{v}_K) \sigma_0^{1/2} - \frac{1}{4} \frac{(1 + \sigma_0)^{1/2} \mp \cos \xi \hat{v}_K \sigma_0^{1/2}}{\hat{\gamma}_K^2 (1 + \sigma_0 - \cos^2 \xi \hat{v}_K^2 \sigma_0)} \right], \quad (17)$$

where the signs + and – stand for the accelerated and decelerated parts, respectively. The angle ξ represents the orientation between the velocity of the plasma outflow and the azimuthal direction in the equatorial plane, as observed in the local rest frame. Here, $\hat{\gamma}_K = (1 - \hat{v}_K^2)^{-1/2}$ and σ_0 denotes the plasma magnetization defined as

$$\sigma_0 \equiv \frac{B^2}{\omega_0}. \quad (18)$$

From the above equation, it can be seen that ϵ_{\pm}^{∞} is determined by a set of five parameters $\{a, B, \omega_0, \xi, r_X\}$, with $r = r_X$ being the radius of the circular orbit (X point).

For energy extraction from the black hole to occur, specific energy extraction conditions must be met. These conditions necessitate that the decelerated portion exhibits negative energy-at-infinity, whereas the accelerated portion must manifest positive energy-at-infinity exceeding both its rest mass and thermal energy, that is

$$\epsilon_{-}^{\infty} < 0, \quad \Delta \epsilon_{+}^{\infty} = \epsilon_{+}^{\infty} - \left(1 - \frac{\Gamma}{\Gamma - 1} \frac{p}{\omega} \right) = \epsilon_{+}^{\infty} > 0. \quad (19)$$

Here plasma is assumed to be relativistically hot with polytropic index $\Gamma = 4/3$.

A. Parameter space analysis

Let us first analyze the influences of the magnetic field B on the energy extraction conditions (19).

In Fig. 4, we show the influence of B on the required orientation angle ξ to satisfy the energy extraction conditions (19) for a near-extreme black hole ($a = 0.99$). Without loss of generality, we set the enthalpy density $\omega_0 = 0.001$ and take the X-point to be at $r_X = r_{\text{ISCO}}^{+}$. From the figure, one can see that for fixed B , $\epsilon_{+}^{\infty} > 0$ is always satisfied, while $\epsilon_{-}^{\infty} < 0$ is only satisfied when ξ is less than some upper bound ξ^c . This is similar to the Kerr case [15], which implies that energy extraction is favored by smaller ξ . As B increases, ξ^c first increases and then decreases. This observation indicates that optimal energy extraction occurs when B takes moderate strength, while energy extraction becomes harder for too small or too large B .

In Fig. 5, we plot the allowed regions in the $a - r_X$ plane where the energy extraction conditions (19) are met for various B . From the figure, one can see that as B increases, the allowed region

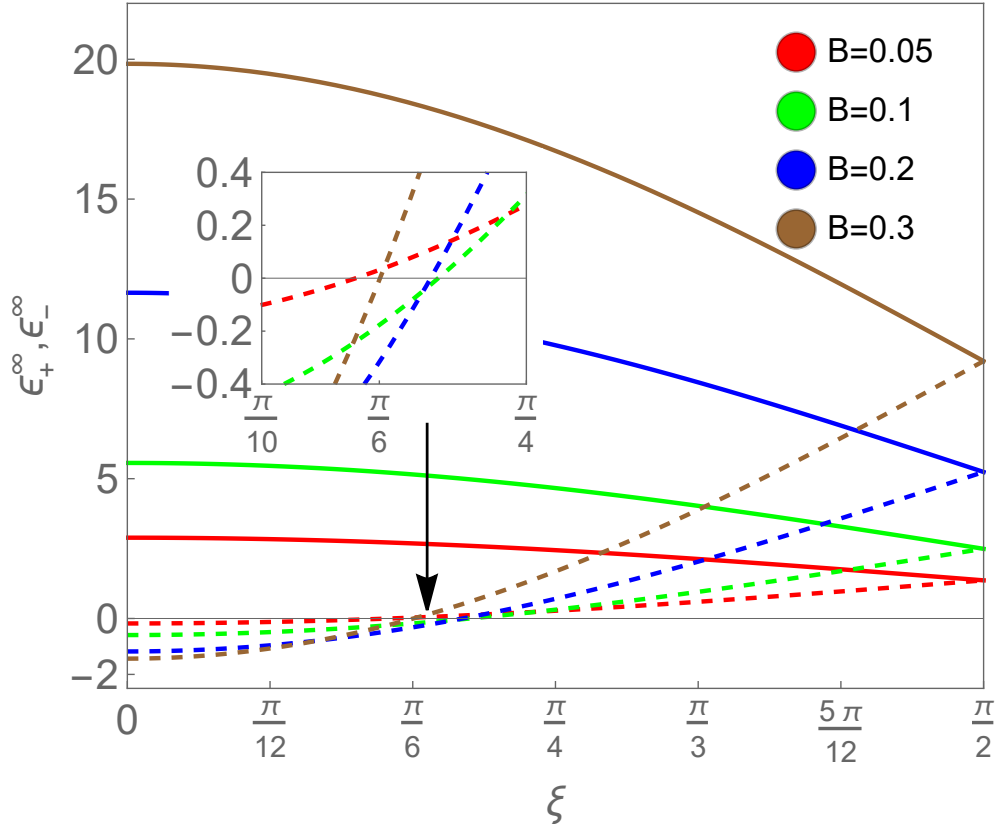


FIG. 4. The energy-at-infinity density ϵ_{\pm}^{∞} as a function of the orientation angle ξ for various B , with $a = 0.99, \omega_0 = 0.001$ and $r_X = r_{\text{ISCO}}^+$. Solid curves are ϵ_+^{∞} while dashed ones are ϵ_-^{∞} . All physical quantities are measured in units of M .

first expands and then shrinks, which once again indicates that a moderate B is most favorable for energy extraction.

B. Energy extraction power and efficiency

To evaluate the feasibility of energy extraction via magnetic reconnection, it is necessary to compute both the power and efficiency of the extraction process. The power $\mathcal{P}_{\text{extr}}$ per unit enthalpy extracted from the black hole can be well estimated as [15]

$$\mathcal{P}_{\text{extr}} = -\epsilon_-^{\infty} A_{\text{in}} U_{\text{in}}, \quad (20)$$

while the efficiency is defined as [15]

$$\eta = \frac{\epsilon_+^{\infty}}{\epsilon_+^{\infty} + \epsilon_-^{\infty}}. \quad (21)$$

The cross-sectional area of the incoming plasma, denoted as A_{in} , can be approximated as $A_{\text{in}} \sim (r_e^2 - r_{\text{ISCO}}^2)$ for highly rotating black holes. The parameter U_{in} is on the order of 10^{-2} and 10^{-1} for

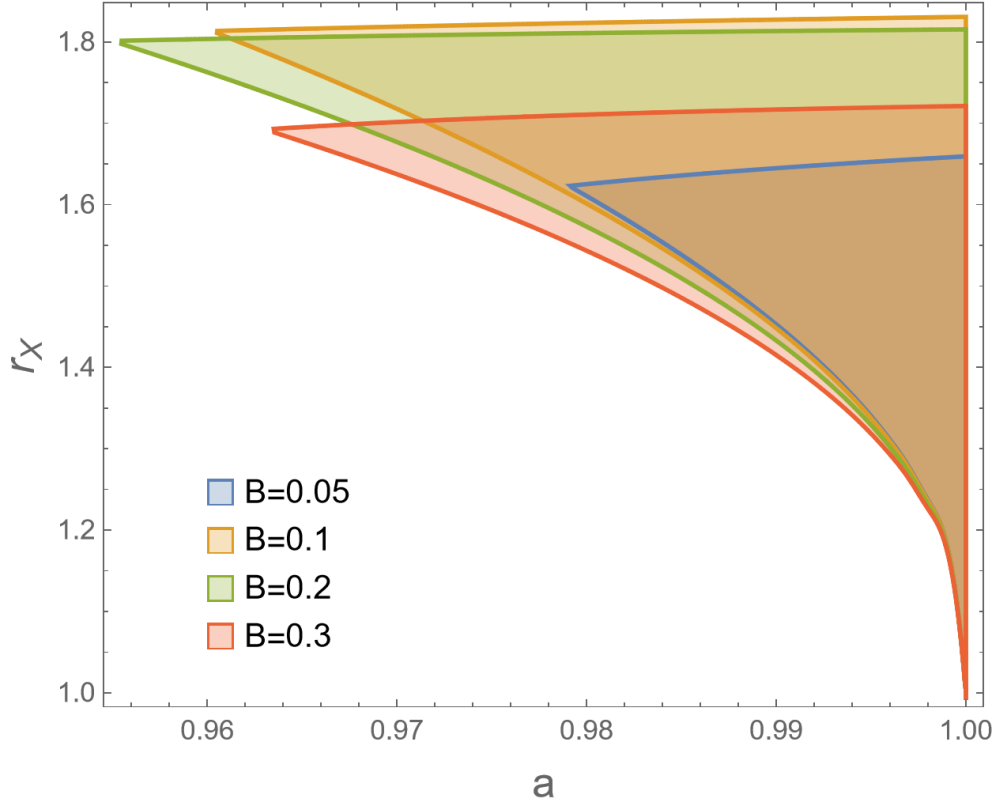


FIG. 5. Allowed regions (shaded) in $a - r_X$ plane where the energy extraction conditions are satisfied for $r_{\text{ISCO}}^+ \leq r_X < r_e$. We set $\xi = \frac{\pi}{12}$ and $\omega_0 = 0.001$. All physical quantities are measured in units of M .

the collisional and collisionless regimes, respectively. If $\eta > 1$, energy is extracted from the black hole.

In Fig. 6, we show a typical picture of the power $\mathcal{P}_{\text{extr}}$ as a function of r_X for various B . For comparison, we also show the Kerr case where the backreaction of the magnetic field on the spacetime is not taken into account. From the figure it can be seen that, with all other parameters fixed, $\mathcal{P}_{\text{extr}}$ is a monotonically decreasing function of r_X , reaching a maximum at $r_X = r_{\text{ISCO}}^+$. As B increases, $\mathcal{P}_{\text{extr}}$ first increases and then decreases, which once again indicates that a moderate B is most favorable for energy extraction. Compared with the Kerr case, we always have a lower power $\mathcal{P}_{\text{extr}}$ in the Kerr-Melvin case. This signifies that the interaction of the magnetic field with spacetime has the potential to impede energy extraction. And the larger B , the stronger this impediment. For example, when $a = 0.99$, the maximum power ratio in the two cases can reach $\frac{\mathcal{P}_{\text{extr}}^{\text{max}}(\text{Kerr-Melvin})}{\mathcal{P}_{\text{extr}}^{\text{max}}(\text{Kerr})} \sim 95\%, 93\%, 74\%, 47\%$ for $B = 0.05, 0.1, 0.2, 0.3$, respectively. Similarly, for $a = 0.998$, $\frac{\mathcal{P}_{\text{extr}}^{\text{max}}(\text{Kerr-Melvin})}{\mathcal{P}_{\text{extr}}^{\text{max}}(\text{Kerr})} \sim 96\%, 93\%, 77\%, 55\%$ for $B = 0.05, 0.1, 0.2, 0.3$, respectively.

In Fig. 7, we show a typical picture of the efficiency η as a function of the X-point location r_X

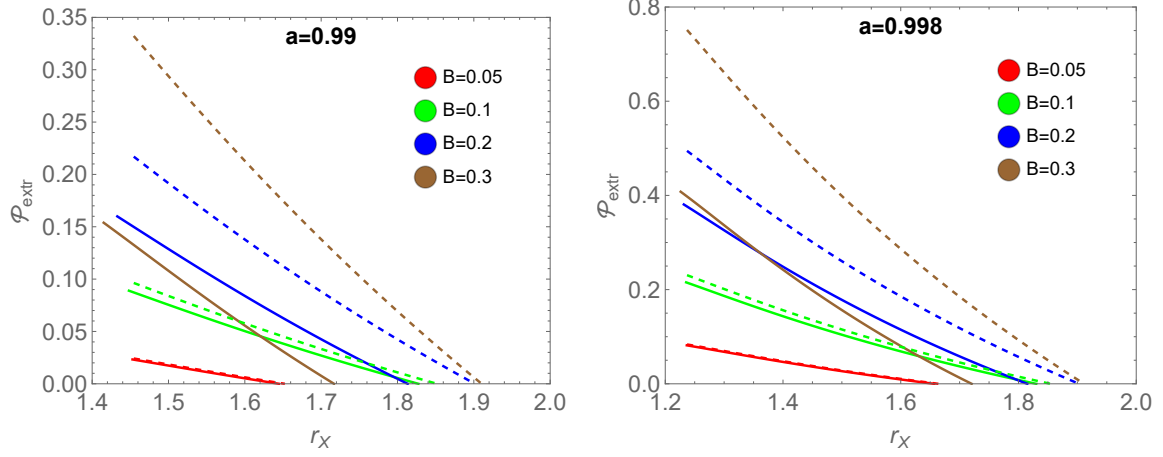


FIG. 6. $\mathcal{P}_{\text{extr}}$ as a function of the X-point location r_X for various B , with $\xi = \frac{\pi}{12}$ and $\omega_0 = 0.001$ and $U_{\text{in}} = 0.1$. r_X is restricted to be in the range $r_{\text{ISCO}}^+ \leq r_X < r_e$. Solid curves are for the Kerr-Melvin case, while dashed ones are the corresponding Kerr case without considering the backreaction of the magnetic field on the spacetime. All physical quantities are measured in units of M .

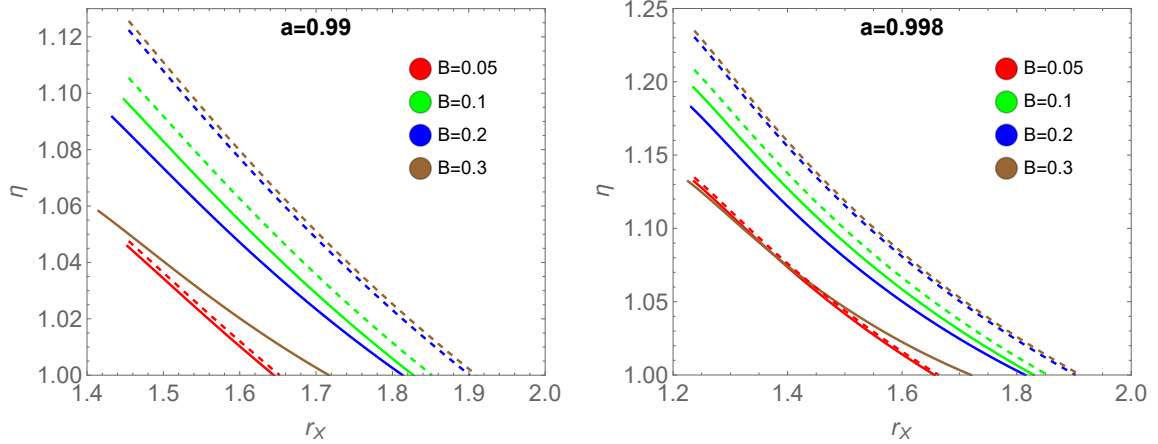


FIG. 7. η as a function of the X-point location r_X for various B , with $\xi = \frac{\pi}{12}$ and $\omega_0 = 0.001$. r_X is restricted to be in the range $r_{\text{ISCO}}^+ \leq r_X < r_e$. Solid curves are for the Kerr-Melvin case, while dashed ones are the corresponding Kerr case without considering the backreaction of the magnetic field on the spacetime. All physical quantities are measured in units of M .

for various B . From the figure, it can be seen that the influence of B on η is similar to its influence on $\mathcal{P}_{\text{extr}}$. As B increases, η first increases and then decreases, again indicating that a moderate B is the most favorable for energy extraction. Compared with the Kerr case, we always have a smaller η in the Kerr-Melvin case. This once again signifies that the interaction of the magnetic field with spacetime has the potential to impede energy extraction. And the larger B , the stronger this impediment. For example, when $a = 0.99$, the maximum efficiency ratio in the two cases

can reach $\frac{\eta^{\max(\text{Kerr-Melvin})}}{\eta^{\max(\text{Kerr})}} \sim 99.8\%, 99.3\%, 97.3\%, 94.0\%$ for $B = 0.05, 0.1, 0.2, 0.3$, respectively. Similarly, for $a = 0.998$, $\frac{\eta^{\max(\text{Kerr-Melvin})}}{\eta^{\max(\text{Kerr})}} \sim 99.7\%, 99.1\%, 96.2\%, 91.7\%$ for $B = 0.05, 0.1, 0.2, 0.3$, respectively.

V. SUMMARY AND CONCLUSIONS

In this study, we revisit the Comisso-Asenjo mechanism [15] by considering the backreaction of the magnetic field on spacetime. The analysis focuses on a fundamental model where the Kerr-Melvin metric describes the local geometry near the horizon. By studying circular orbits in the equatorial plane, evaluating energy extraction conditions, power and efficiency of the energy extraction, we found the significant influence of the backreaction on the process.

The magnetic field B exerts a significant influence on the geometry of black holes, impacting both the ergoregion and the surrounding orbits. A stronger magnetic field results in a reduction of the ergoregion in the equatorial plane where magnetic reconnection occurs, as illustrated in Fig. 1. There is a critical value for the magnetic field strength $B = B_c$, beyond which circular orbits cease to exist in the equatorial plane, as shown in Fig. 2. The value of B_c rises with the black hole spin a , and in the extreme limit $a \rightarrow 1$, $B_c \sim 0.57$. Consequently, if $B > 0.57$, magnetic reconnection cannot take place in the current scenario. As shown in Fig. 3, only when a exceeds some extremely high value a_c can r_{ISCO}^+ enter the ergoregion. For example, $a_c \sim 0.943, 0.939, 0.934, 0.935$ for $B = 0, 0.1, 0.2, 0.3$, respectively. It can be seen that with the increase of B , a_c first decreases and then increases.

This effect of magnetic fields on spacetime geometry further affects energy extraction. As B increases, the required minimal orientation angle ξ to satisfy the energy extraction conditions (19) first increases and then decreases, as shown in Fig. 4. Additionally, with increasing B , the allowed region in the $a - r_X$ plane to meet the energy extraction conditions first expands and then shrinks, as shown in Fig. 5.

Upon analyzing the power $\mathcal{P}_{\text{extr}}$ and efficiency η of energy extraction as illustrated in Figs. 6 and 7, it was observed that both quantities exhibit an initial increase followed by a decrease with the rise of B . The values consistently remain noticeably lower than their Kerr counterparts, showing a more significant decrease as B increases.

All these results imply that while a stronger magnetic field enhances plasma magnetization, thereby promoting energy extraction, its backreaction on spacetime poses challenges. The interplay between these factors indicates that a moderate magnetic field strength is most conducive to energy

extraction. Notably, there is a maximum limit for the magnetic field strength B_c linked to the black hole spin parameter a , beyond which circular orbits are restricted, hindering energy extraction in the current scenario. Nevertheless, it is important to acknowledge that energy extraction may still be achieved through alternative orbits like elliptic orbits or those not confined to the equatorial plane.

We utilized the Kerr-Melvin metric in this study to elucidate the backreaction of the magnetic field on the black hole's geometry. While this model offers a simplified perspective, it aids in comprehending the influences of the magnetic field on the Comisso-Asenjo mechanism to a certain degree. However, in more realistic astrophysical scenarios, the incorporation of intricate models or relativistic magnetohydrodynamics is essential to depict the interplay between black holes and magnetic fields accurately, which calls for further investigations.

ACKNOWLEDGMENTS

This work is supported by the National Natural Science Foundation of China (NNSFC) under Grant No 12075207.

-
- [1] D. Christodoulou, "Reversible and irreversible transformations in black hole physics," *Phys. Rev. Lett.* **25** (1970) 1596–1597.
 - [2] J. M. Bardeen, W. H. Press, and S. A. Teukolsky, "Rotating black holes: Locally nonrotating frames, energy extraction, and scalar synchrotron radiation," *Astrophys. J.* **178** (1972) 347.
 - [3] R. M. Wald, "Energy Limits on the Penrose Process," *Astrophys. J.* **191** (1974) 231.
 - [4] S. A. Teukolsky and W. H. Press, "Perturbations of a rotating black hole. III - Interaction of the hole with gravitational and electromagnetic radiation," *Astrophys. J.* **193** (1974) 443–461.
 - [5] T. Piran, J. Shaham, and J. Katz, "High efficiency of the penrose mechanism for particle collisions," *Astrophys. J. Lett.* **196** (1975) L107.
 - [6] R. D. Blandford and R. L. Znajek, "Electromagnetic extractions of energy from Kerr black holes," *Mon. Not. Roy. Astron. Soc.* **179** (1977) 433–456.
 - [7] M. Takahashi, S. Nitta, Y. Tatematsu, and A. Tomimatsu, "Magnetohydrodynamic Flows in Kerr Geometry: Energy Extraction from Black Holes," *Astrophys. J.* **363** (Nov., 1990) 206.
 - [8] H. K. Lee, R. A. M. J. Wijers, and G. E. Brown, "The Blandford-Znajek process as a central engine for a gamma-ray burst," *Phys. Rept.* **325** (2000) 83–114, [arXiv:astro-ph/9906213](https://arxiv.org/abs/astro-ph/9906213).
 - [9] A. Tchekhovskoy, J. C. McKinney, and R. Narayan, "Simulations of Ultrarelativistic

- Magnetodynamic Jets from Gamma-ray Burst Engines,” *Mon. Not. Roy. Astron. Soc.* **388** (2008) 551, [arXiv:0803.3807 \[astro-ph\]](#).
- [10] S. S. Komissarov and M. V. Barkov, “Activation of the Blandford-Znajek mechanism in collapsing stars,” *Mon. Not. Roy. Astron. Soc.* **397** (2009) 1153, [arXiv:0902.2881 \[astro-ph.HE\]](#).
- [11] J. C. McKinney and C. F. Gammie, “A Measurement of the electromagnetic luminosity of a Kerr black hole,” *Astrophys. J.* **611** (2004) 977–995, [arXiv:astro-ph/0404512](#).
- [12] J. F. Hawley and J. H. Krolik, “Magnetically driven jets in the Kerr metric,” *Astrophys. J.* **641** (2006) 103–116, [arXiv:astro-ph/0512227](#).
- [13] S. S. Komissarov and J. C. McKinney, “Meissner effect and Blandford-Znajek mechanism in conductive black hole magnetospheres,” *Mon. Not. Roy. Astron. Soc.* **377** (2007) L49–L53, [arXiv:astro-ph/0702269](#).
- [14] A. Tchekhovskoy, R. Narayan, and J. C. McKinney, “Efficient Generation of Jets from Magnetically Arrested Accretion on a Rapidly Spinning Black Hole,” *Mon. Not. Roy. Astron. Soc.* **418** (2011) L79–L83, [arXiv:1108.0412 \[astro-ph.HE\]](#).
- [15] L. Comisso and F. A. Asenjo, “Magnetic reconnection as a mechanism for energy extraction from rotating black holes,” *Phys. Rev. D* **103** no. 2, (2021) 023014, [arxiv:2012.00879 \[astro-ph.HE\]](#).
- [16] S. Koide and K. Arai, “Energy extraction from a rotating black hole by magnetic reconnection in ergosphere,” *Astrophys. J.* **682** (2008) 1124, [arxiv:0805.0044 \[astro-ph\]](#).
- [17] K. Parfrey, A. Philippov, and B. Cerutti, “First-Principles Plasma Simulations of Black-Hole Jet Launching,” *Phys. Rev. Lett.* **122** no. 3, (2019) 035101, [arXiv:1810.03613 \[astro-ph.HE\]](#).
- [18] S. S. Komissarov, “Observations of the Blandford-Znajek and the MHD Penrose processes in computer simulations of black hole magnetospheres,” *Mon. Not. Roy. Astron. Soc.* **359** (2005) 801–808, [arXiv:astro-ph/0501599](#).
- [19] W. E. East and H. Yang, “Magnetosphere of a spinning black hole and the role of the current sheet,” *Phys. Rev. D* **98** no. 2, (2018) 023008, [arXiv:1805.05952 \[astro-ph.HE\]](#).
- [20] B. Ripperda, F. Bacchini, and A. Philippov, “Magnetic Reconnection and Hot Spot Formation in Black Hole Accretion Disks,” *Astrophys. J.* **900** no. 2, (2020) 100, [arXiv:2003.04330 \[astro-ph.HE\]](#).
- [21] L. Comisso, M. Lingam, Y.-M. Huang, and A. Bhattacharjee, “General theory of the plasmoid instability,” *Physics of Plasmas* **23** no. 10, (2016) 100702, [arxiv:1608.04692 \[astro-ph, physics:math-ph, physics:physics\]](#).
- [22] D. A. Uzdensky, N. F. Loureiro, and A. A. Schekochihin, “Fast magnetic reconnection in the plasmoid-dominated regime,” *Phys. Rev. Lett.* **105** (2010) 235002, [arxiv:1008.3330 \[astro-ph.SR\]](#).
- [23] L. Comisso, M. Lingam, Y.-M. Huang, and A. Bhattacharjee, “Plasmoid instability in forming current sheets,” *Astrophys. J.* **850** no. 2, (2017) 142, [arxiv:1707.01862 \[astro-ph.HE\]](#).
- [24] W. Daughton, V. Roytershteyn, B. J. Albright, H. Karimabadi, L. Yin, and K. J. Bowers, “Transition from collisional to kinetic regimes in large-scale reconnection layers,” *Phys. Rev. Lett.* **103** no. 6,

- (2009) 065004.
- [25] A. Bhattacharjee, Y.-M. Huang, H. Yang, and B. Rogers, “Fast reconnection in high-lundquist-number plasmas due to secondary tearing instabilities,” *Physics of Plasmas* **16** no. 11, (2009) 112102, [arXiv:0906.5599 \[physics\]](#).
- [26] K. Mori *et al.*, “NuSTAR discovery of a 3.76-second transient magnetar near Sagittarius A*,” *Astrophys. J. Lett.* **770** (2013) L23, [arXiv:1305.1945 \[astro-ph.HE\]](#).
- [27] J. A. Kennea *et al.*, “Swift Discovery of a New Soft Gamma Repeater, SGR J1745-29, near Sagittarius A*,” *Astrophys. J. Lett.* **770** (2013) L24, [arXiv:1305.2128 \[astro-ph.HE\]](#).
- [28] R. P. Eatough *et al.*, “A strong magnetic field around the supermassive black hole at the centre of the Galaxy,” *Nature* **501** (2013) 391–394, [arXiv:1308.3147 \[astro-ph.GA\]](#).
- [29] S. A. Olausen and V. M. Kaspi, “The McGill Magnetar Catalog,” *Astrophys. J. Suppl.* **212** (2014) 6, [arXiv:1309.4167 \[astro-ph.HE\]](#).
- [30] **Event Horizon Telescope** Collaboration, K. Akiyama *et al.*, “First M87 Event Horizon Telescope Results. VIII. Magnetic Field Structure near The Event Horizon,” *Astrophys. J. Lett.* **910** no. 1, (2021) L13, [arXiv:2105.01173 \[astro-ph.HE\]](#).
- [31] S.-W. Wei, H.-M. Wang, Y.-P. Zhang, and Y.-X. Liu, “Effects of tidal charge on magnetic reconnection and energy extraction from spinning braneworld black hole,” *JCAP* **04** no. 04, (2022) 050, [arXiv:2201.12729 \[gr-qc\]](#).
- [32] W. Liu, “Energy extraction via magnetic reconnection in the ergosphere of a rotating non-kerr black hole,” *Astrophys. J.* **925** no. 2, (2022) 149, [arXiv:2204.07338 \[astro-ph.HE\]](#).
- [33] A. Carleo, G. Lambiase, and L. Mastrototaro, “Energy extraction via magnetic reconnection in lorentz breaking kerr–sen and kiselev black holes,” *Eur. Phys. J. C* **82** no. 9, (2022) 776, [arXiv:2206.12988 \[gr-qc\]](#).
- [34] M. Khodadi, “Magnetic reconnection and energy extraction from a spinning black hole with broken lorentz symmetry,” *Phys. Rev. D* **105** no. 2, (2022) 023025, [arXiv:2201.02765 \[gr-qc\]](#).
- [35] Z. Li, X.-K. Guo, and F. Yuan, “Energy extraction from rotating regular black hole via comisso-asenjo mechanism,” *Phys. Rev. D* **108** no. 4, (2023) 044067, [arXiv:2304.08831 \[gr-qc\]](#).
- [36] Z. Li and F. Yuan, “Energy extraction via comisso-asenjo mechanism from rotating hairy black hole,” *Phys. Rev. D* **108** no. 2, (2023) 024039, [arXiv:2304.12553 \[gr-qc\]](#).
- [37] M. Khodadi, D. F. Mota, and A. Sheykhi, “Harvesting energy driven by comisso-asenjo process from kerr-mog black holes,” *JCAP* **10** (2023) 034, [arXiv:2307.00478 \[astro-ph.HE\]](#).
- [38] S. Shaymatov, M. Alloqulov, B. Ahmedov, and A. Wang, “A kerr-newman-mog black hole’s impact on the magnetic reconnection,” *arXiv:2307.03012 [gr-qc]* (2023) , [arXiv:2307.03012 \[gr-qc\]](#).
- [39] C.-H. Wang, C.-Q. Pang, and S.-W. Wei, “Extracting energy via magnetic reconnection from kerr–de sitter black holes,” *Phys. Rev. D* **106** no. 12, (2022) 124050, [arXiv:2209.08837 \[gr-qc\]](#).
- [40] S.-J. Zhang, “Energy extraction via magnetic reconnection in Konoplya-Rezzolla-Zhidenko parametrized black holes,” *Phys. Rev. D* **109** no. 8, (2024) 084066, [arXiv:2402.15050 \[gr-qc\]](#).

- [41] B. Chen, Y. Hou, J. Li, and Y. Shen, “Energy Extraction from a Kerr Black Hole via Magnetic Reconnection within the Plunging Region,” [arXiv:2405.11488 \[gr-qc\]](#).
- [42] R. M. Wald, “Black hole in a uniform magnetic field,” *Phys. Rev. D* **10** (1974) 1680–1685.
- [43] F. J. Ernst, “Black holes in a magnetic universe,” *J. Math. Phys.* **17** no. 1, (1976) 54–56.
- [44] F. J. Ernst and W. J. Wild, “Kerr black holes in a magnetic universe,” *J. Math. Phys.* **17** no. 2, (1976) 182.
- [45] G. W. Gibbons, A. H. Mujtaba, and C. N. Pope, “Ergoregions in Magnetised Black Hole Spacetimes,” *Class. Quant. Grav.* **30** no. 12, (2013) 125008, [arXiv:1301.3927 \[gr-qc\]](#).
- [46] Z. Budinova, M. Dovciak, V. Karas, and A. Lanza, “Magnetic fields around black holes,” [arXiv:astro-ph/0005216](#).
- [47] J. Bičák, V. Karas, and T. Ledvinka, “Black holes and magnetic fields,” *IAU Symp.* **238** (2007) 139–144, [arXiv:astro-ph/0610841](#).
- [48] G. W. Gibbons, Y. Pang, and C. N. Pope, “Thermodynamics of magnetized Kerr-Newman black holes,” *Phys. Rev. D* **89** no. 4, (2014) 044029, [arXiv:1310.3286 \[hep-th\]](#).
- [49] M. Astorino, G. Compère, R. Oliveri, and N. Vandevoorde, “Mass of Kerr-Newman black holes in an external magnetic field,” *Phys. Rev. D* **94** no. 2, (2016) 024019, [arXiv:1602.08110 \[gr-qc\]](#).
- [50] I. Booth, M. Hunt, A. Palomo-Lozano, and H. K. Kunduri, “Insights from Melvin–Kerr–Newman spacetimes,” *Class. Quant. Grav.* **32** no. 23, (2015) 235025, [arXiv:1502.07388 \[gr-qc\]](#).
- [51] M. Astorino, “Magnetised Kerr/CFT correspondence,” *Phys. Lett. B* **751** (2015) 96–106, [arXiv:1508.01583 \[hep-th\]](#).
- [52] M. Astorino, “Thermodynamics of Regular Accelerating Black Holes,” *Phys. Rev. D* **95** no. 6, (2017) 064007, [arXiv:1612.04387 \[gr-qc\]](#).
- [53] Y. Gao and S. Gao, “Testing the weak cosmic censorship conjecture for extremal magnetized Kerr–Newman black holes,” *Eur. Phys. J. C* **82** no. 8, (2022) 763, [arXiv:2208.00703 \[gr-qc\]](#).
- [54] M. Wang, S. Chen, and J. Jing, “Kerr black hole shadows in Melvin magnetic field with stable photon orbits,” *Phys. Rev. D* **104** no. 8, (2021) 084021, [arXiv:2104.12304 \[gr-qc\]](#).
- [55] Y. Hou, Z. Zhang, H. Yan, M. Guo, and B. Chen, “Image of a Kerr-Melvin black hole with a thin accretion disk,” *Phys. Rev. D* **106** no. 6, (2022) 064058, [arXiv:2206.13744 \[gr-qc\]](#).
- [56] C. Chakraborty, P. Patil, and G. Akash, “Magnetic Penrose process in the magnetized Kerr spacetime,” *Phys. Rev. D* **109** no. 6, (2024) 064062, [arXiv:2401.13347 \[astro-ph.HE\]](#).
- [57] A. N. Aliev and D. V. Galtsov, “Magnetized Black Holes,” *Sov. Phys. Usp.* **32** (1989) 75.
- [58] A. N. Aliev and D. V. Galtsov, “Exact Solutions For Magnetized Black Holes,” *Astrophys. Space Sci.* **155** (1989) 181.
- [59] M. A. Melvin, “Pure magnetic and electric geons,” *Phys. Lett.* **8** (1964) 65–70.
- [60] D. V. Galtsov and V. I. Petukhov, “Black Hole in an External Magnetic Field,” *Zh. Eksp. Teor. Fiz.* **74** (1978) 801–818.